ROBUST FILTERING OF GHOST AND PEG-LEG FROM SEA FLOOR SEISMIC DATA

Raoni de Carvalho Costa Alves [1] and Sergio Adriano Moura Oliveira [2]

[1]Petrobras, Rio de Janeiro, RJ, Brazil

[2]Universidade Estadual do Norte Fluminense – UENF, LENEP, Macaé, RJ, Brazil

ABSTRACT. The processing of compressional waves from the acoustic components of ocean bottom seismic data is performed decomposing the compressional wavefield on its upgoing an downgoing components, treating the first order multiples, composed by the overlap between the receiver ghost and peg-leg. The separation of these wavefields is achieved through the adaptive summation of the hydrophone and geophone components, usually on a least square sense. This method of separation is known as PZ summation, because it involves an operation between pressure and vertical particle velocity measurements. However, due to the difference in response of the pressure and velocity sensors, the premises assumed on the least square summation can be violated, degrading the results. To overcome these difficulties, a more robust method can be achieved using the L_1 norm criterion for the adaptive sum. A comparison was made between the results obtained with the Iterative Reweighted Least Squares and Wiener-Levinson filters. The robustness of the L_1 norm sum was demonstrated by applications on PZ summation of Ocean Bottom Cable data from the Jubarte area, in the Campos Basin, Brazil, showing improvements, especially when the multiples are present in the estimation window used to derive the filter coefficients.

Keywords: PZ summation; Wiener-Levinson; IRLS; ghost; peg-leg

INTRODUCTION

Multi-component seafloor seismic have been used as a successful technique to improve the reservoir monitoring. This type of acquisition can increase the fold under production facilities obstacles, as well as wide the azimuthal illumination and measure the converted shear wavefield. However, the processing flow for Ocean Bottom Cable (OBC) and Ocean Bottom Nodes (OBN) data differs from conventional streamer data mainly due the difference between source and receiver depths which provides an asymmetric raypath.

A method to process the hydrophone and geophone data from multi-component seismic survey was presented by Amundsen and Reitan (1995) and Soubaras (1996). Later Beresford and Janex (1996), Verschuur et al. (2003), Muijs et al. (2007), Wang and Grion (2008), Edme and Singh (2009), and Hugonnet et al. (2011), addressed the theme of the ocean bottom seismic (OBS) data processing, explaining methods to separate the wavefield components under the receiver domain as well as their application in a real-world situation.

This paper concentrates on the acoustic wavefield immediately above the water bottom surface, under a unidimensional approach. Hugonnet et al. (2011), summarized the aspects of the hydrophone and geophone processing, based on Soubaras (1996), and called it as PZ summation (pressure with vertical particle velocity), generalizing it to the three-dimensional notation, under the least square

sense. However, Guitton and Verschuur (2004), explain that under non-gaussian distribution, when the multiple energy is present in the considered time window, the least square method provides poor adaptive sum to multiple attenuation, once that is highly affected by spurious measures, and suggest the use of the L_1 norm.

We propose to apply a linear convolutional adapting filter based in the L_1 norm instead of the least square filter in the formulation of the PZ summation, to accomplish a unidimensional robust acoustic decomposition, separating the upgoing and downgoing wave fields, to treat the receiver ghost, and to provide inputs to address the peg-leg multiple on the surveyed seafloor PP seismic data. The IRLS (Iterative Reweighted Least Squares) algorithm (Scales and Gersztenkorn, 1988) was used to obtain the filter coefficients and it was applied to PZ summation on OBC Seismic data from Jubarte area, in the north of the Campos Basin, on the Espírito Santo coast, Brazil. A short explanation about the fundamentals of the least square and L_1 norm filtering is showed. We also show the summarized formulation of the unidimensional PZ summation and the modification proposed in the adaptive sums.

METHODS

The measured wavefields

In conventional streamer acquisition, the receiver is commonly located few meters under the free- air surface, so the receiver side ghost notches contaminate only the low and the high frequency bands on the acquired data, affecting the data resolution. In ocean bottom acquisition, the noticeable depth of the receiver, related to free-air surface, provides ghost notches interference on the useful central band of the seismic data. The ghost arrives on the receiver in the downward direction, however there is a synchronic event measured that arrives in the upward direction on the receiver, and it is called peg-leg (Soubaras, 1996; Hugonnet et al., 2011). The overlap between them provides the water column delayed multiple event, measured in a sea-floor seismic survey. In terms of primary waves, to rightly process them, it is required separate the wavefield in its upgoing and downgoing components from the hydrophone and the vertical geophone component receivers.

We can see in the Figures 1 and 2 some events measured in a sea-floor seismic survey, with the depth of z, represented by a source S, x away from the hydrophone H and the vertical geophone G on the same receiver location, under a bidimensional case. In the Figure 1, the simplified upgoing wavefield component is showed, exposing the peg-leg trace set as the dashed rays from water bottom and the deep reflector. In the simplified downgoing wavefield (Figure 2) the ghost trace set is represented as the dashed rays from water bottom and the deep reflector.

We can approximate this situation to a unidimensional case, showed in Figure 3. The letters D and U respectively represents the downward and upward arriving wavefields, while the subscripted d, wb, g, pg and p are, respectively, direct wave, water-bottom primary reflection, the ghost, the peg-leg

and the deep primary reflections. Thus, the Figure 3 illustrates the immediately above the water-bottom acoustic decomposition, the subscript *p* refers to the possibility of the approximation be expanded if we consider the acoustic media. This simplification can be applied to deep reflectors because the small source-receiver offset per target depth ratio allows an unidimensional treatment. The Figures 1, 2 and 3 highlights the ghost and the peg-leg events as the dashed lines and vectors because those are considered as noises that compound the first order multiples in the sea-floor seismic data, when we follow the upgoing wavefield processing strategy, on which was focused this search. For downgoing wavefield processing strategy, the ghost is separated into the downgoing wavefield and it is considered as signal to accomplish the called mirror migration (Pacal et al., 2015).
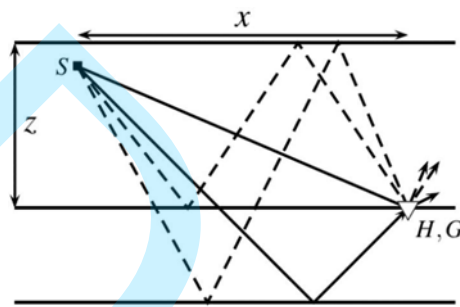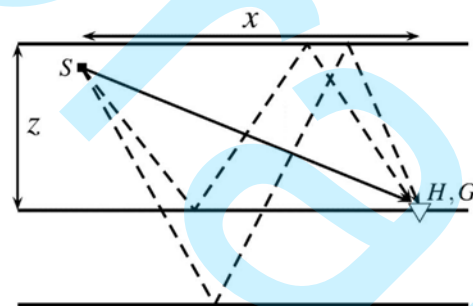
Figure 1 - *Upgoing wavefield.*

Figure 2 - *Downgoing wavefield.*

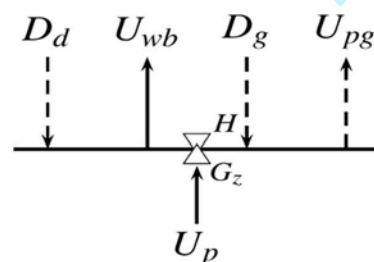**Figure 3 -** *Unidimensional acoustic decomposition to sea- floor seismic data.*

The pressure with vertical particle velocity summation

To treat the receiver ghost and peg-leg in ocean bottom multi-component seismic data, following the upgoing processing guideline, Hugonnet et al. (2011) summarized the formulation of PZ summation based on Soubaras (1996) by setting

$$U = H + f_0 * G \tag{1}$$

$$D = H - f_0 * G \tag{2}$$

where U and D are respectively upgoing and downgoing wavefields, H and G are hydrophone and geophone data components, and $f_0 = argmin \, | \, IH' - f * G'I|^2_2$ is the least square filter. The elements H' and G' are defined in the equation (4) and (5). The filter with the regularizing whitenoise λ (Yilmaz, 2001) is given by

$$\tag{3}$$

$$f_0 = [G'^T G^1 + \lambda I]^{-1} G'^T H^1,$$

which can be numerical solved by the Wiener-Levinson (W-L) algorithm (Golub and Van Loan, 1996; Rosa, 2018).

The adaptive sum is applied due to differences between hydrophone (Figure 4) and geophone (Figure 5) signals, related mainly to coupling and its scalar and vector measures which provide an orthogonal phase delay between them. In addition, because of the polarizing feature of the geophone, the notches from the receiver ghost appear on the amplitude spectra with opposite peaks and troughs on hydrophone and geophone components (Figure 6). To show a qualitative presentation for the synthetic trace modeling, the ghost amplitude was not attenuated by the geometrical spreading. The ghost is detected at three times the time of the primary event in the Figures 4 and 5, so the peg-leg overlaps it with a magnitude equal to the square power ghost amplitude, amplifying the amplitude level
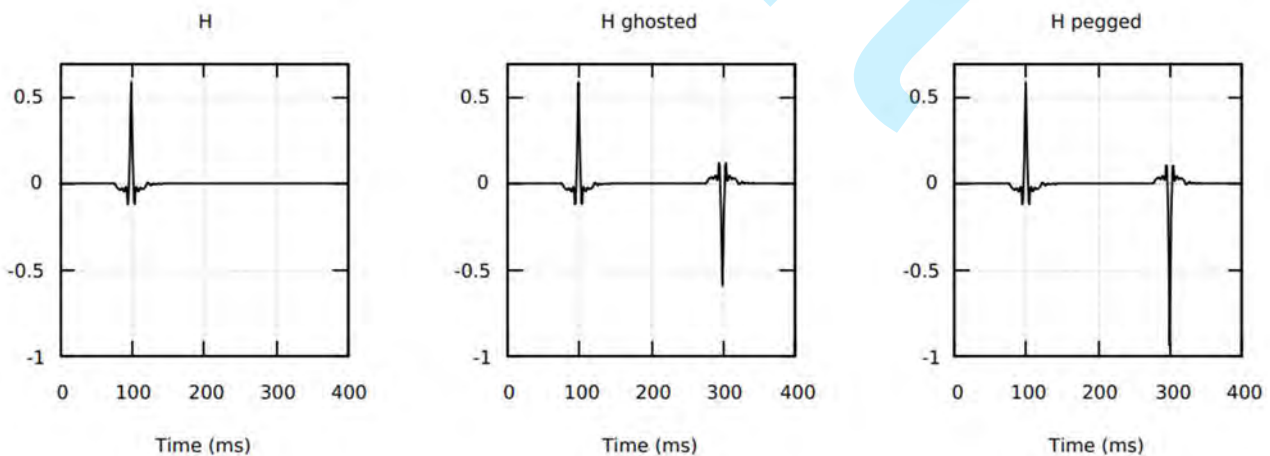

Figure 4 – *Hydrophone trace simulating. From left to right: primary event, ghost and peg leg overlapping the ghost.*
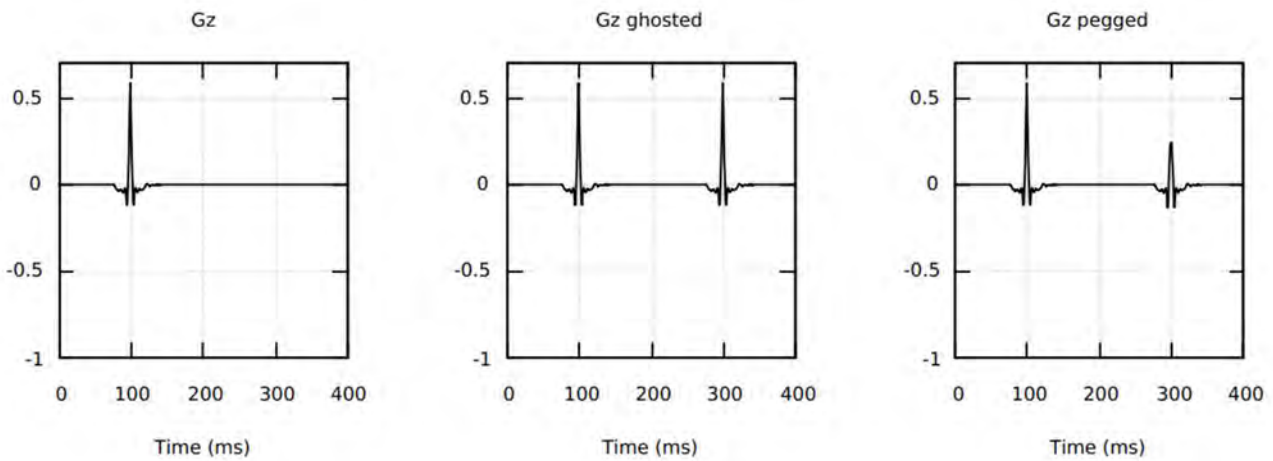
Figure 5 – *Vertical geophone trace simulating. From left to right: the primary event, ghost and peg-leg overlapping the ghost.*

of the multiple in the hydrophone and reducing the one in the geophone. The assumptions to build the traces from the upgoing and downgoin wavefields is found in Soubaras (1996).
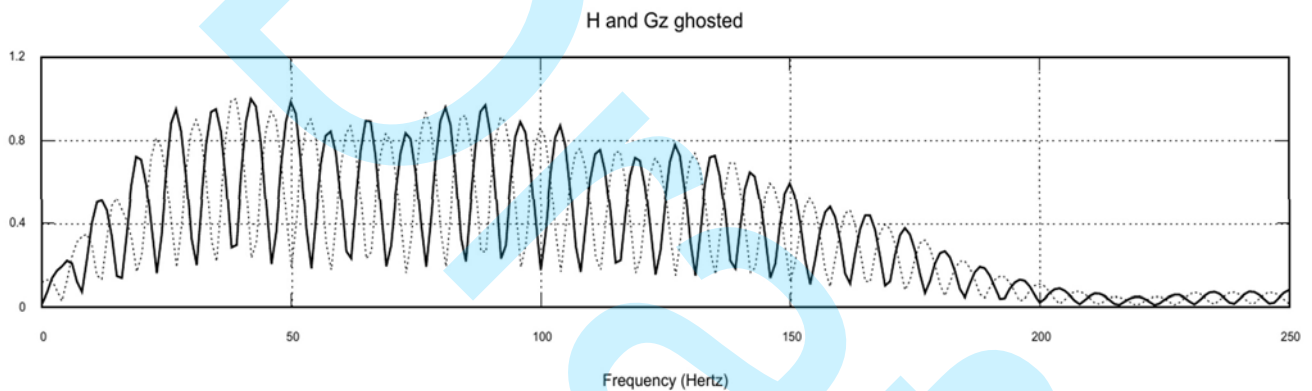

Figure 6 – *Normalized amplitude spectra for the synthetic hydrophone as the continuous black line, and the geophone as the dashed line, contaminated by its receiver ghost. Note the alternating notches.*

To compensate that effect, Soubaras (1996) proposed the crossghosting operation preceding the filter calculation, making

$$H' = g_0 * H, \qquad (4)$$

$$G' = h_0 * G, \qquad (5)$$

where h_0 and g_0 are respectively the deterministic first order hydrophone and geophone ghost operators, which were built in time domain considering the normal incidence angle $(\theta = 0)$ and time delay as $\Delta t = 2z \cos\theta/v$ (Figure 7). The
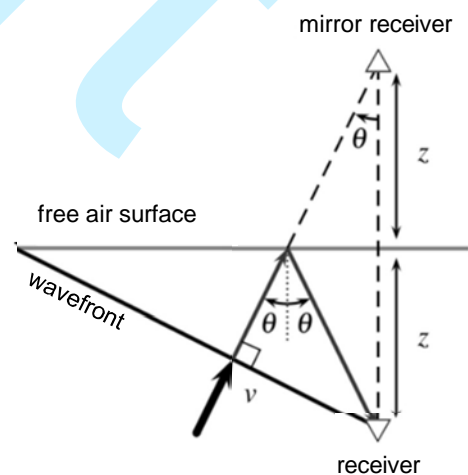

Figure 7 - *Associated geometry to receiver ghost delay. Adapted from Rosa (2018).*

reflectivity r from free air surface which is about -1, the water column velocity v by around 1500 meters per second and the geometric spreading coefficient E, by around 0.98 (Rosa, 2018), providing us

$$h_0 = \delta_t - rE\delta_{t-\Delta t} \tag{6}$$

$$g_0 = \delta_t + rE\delta_{t-\Delta t}, \tag{7}$$

where δ_t is the delta function.

To attenuation of the peg-leg, we have the adaptive sum

$$P = U - p_0 * D, \tag{8}$$

where P is the un-pegged data, U and D are respectively the upgoing and downgoing wavefields from deghosting, and

$$p_0 = [D^TD + \lambda I]^{-1}D^TU, \tag{9}$$

is the least square predictive filter, once the downgoing is a delayed version of the upgoing wavefield (Soubaras, 1996; Ang et al., 2010; Edme and Singh, 2009; Hugonnet et al., 2011).

The Robust PZ summation

With the crossghosting operation and the IRLS method stated (Appendix), we propose a small modification on formulation of the acoustic decomposition, substituting the least square filter by the L_1 norm-based filter obtained by IRLS, for this we have that

$$U = H + f_k * G \tag{10}$$

$$D = H - f_k * G, \tag{11}$$

where

$$f_k = argmin \; ||H' - f * G'||^1 \quad {}_1 \tag{12}$$

is now the filter given by

$$f_k = [G'^TAG^1 + \mu B]^{-1}G'^TAH' \,, \tag{13}$$

which was solved by Cholesky factorization (Golub and Van Loan, 1996) because the system matrix is positive definite (Li et al., 2016). In this case, we have the modeling deviation as

$$\Delta = H' - f_{k-1} * G'. \tag{14}$$

The parameter μ refer to the system matrix regularization. Note that **A** and **B** are the IRLS method system matrices described in the appendix by equations A3 and A5, in which there is a parameter ε that controls the L_1 norm approximation accuracy.

A similar formulation can be developed to the depeglegging, so that

$$P = U - p_k * D,\qquad(15)$$

where the predictive filter is

$$p_k = [D^T A D + \mu B]^{-1} D^T A U,\qquad(16)$$

however, in this case, the modeling deviation is

$$\Delta = U - p_{k-1} * D.\qquad(17)$$

Note that **A** and **B** are built now from the new modeling deviation given by equation 17.

Data preconditioning – Designature

The method was applied to the hydrophone and the accelerometer of the OBC data 0364_4D_JUBARTE_PRM_MONITOR_ 01 from Jubarte area in the north of the Campos Basin. A receiver line parallel and close to a shot line, to simulate a bidimensional survey and evaluate the method on the receiver stacked lines and the receiver gathers from the real data.

Before submitting the data to the robust PZ summation, a designature processing was applied, using a statistically derived wavelet estimated from the flattened water bottom from the receiver stacked line, to calculate the predictive filter to debubbling and an equivalent zero phase wavelet. After designature, the data was resampled to 4 milliseconds, the half of original input sample rate and submitted to anti-alias filtering.

The hydrophone was low cut filtered to attenuate anomalous low frequency band, and the accelerometer was integrated to simulate the geophone data, once the particle acceleration is the derivative of the particle velocity.

Data processing – Deghosting

The deghosting process was divided in two steps: filter calculation and filter application on receiver gather. During the first step, just one filter is calculated for each receiver gather, using an estimation window on the near receiver stacked section of each component, which is detailed in the

Figure 8. Note on the Figure 8, there are some relative anomalous amplitude noise over the stacked vertical component. Therefore, the level of the amplitude for the hydrophone component is four orders of the magnitude greater than the geophone, thus, the integrated accelerometer was gain calibrated to stablish the numerical operations during the filter calculation. The sum ran on the hydrophone and the vertical geophone receiver stacked sections, to evaluate the filter quality. After the calculation, the filter was applied on the whole receiver gather traces and the trace to trace sum ran before the stack. The filter quality was evaluated on both, gathers and stacked sections. We used two sizes for the estimating window on the receiver stack sections, a long, between 0.0 and 10.0 seconds, and a short, between 1.06 and 2.48 seconds, and the results were evaluated.
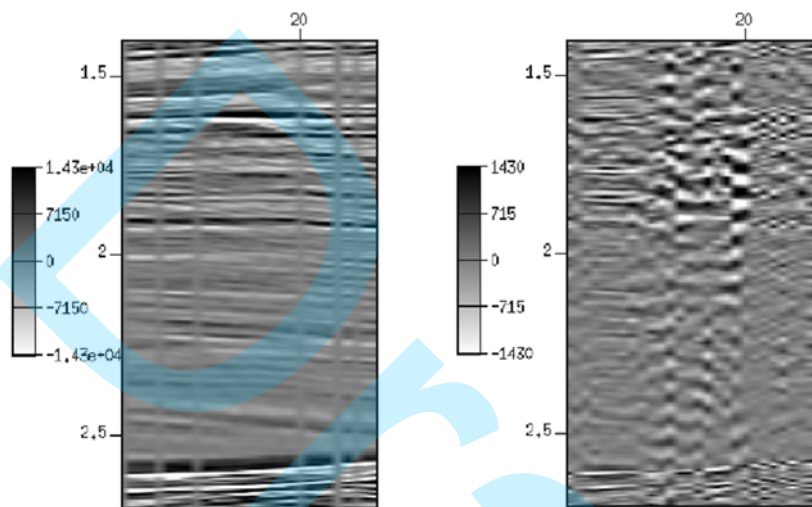

Figure 8 - *Details on long window deghosting receiver stack lines. From left to right are the input designatured filtered hydrophone and the input designatured integrated vertical accelerometer.*

Data processing – Depeglegging

A trace to trace short predictive filtering was accomplish to do the attenuation of the peg-leg, using the IRLS short window outputs from deghost process as the input data. The upgoing and downgoing receiver gathers were submitted to the adaptive sum, providing the unpegged data. After the filtering, the receiver gathers were stacked providing the receiver stack lines.

RESULTS

Deghosting – long window

The crossghosting was applied before the filter calculation due to the multiple events contained in the long estimation window. The multiple energy inserts spurious conditions violating least squares premises. The results on stacked receiver lines, during the filter calculation step, verified the robustness of the IRLS filtering over the Wiener-Levinson filtering.

Though the results observed on stacked receiver lines, when the method was applied on the receiver gathers (Figure 9), artifacts contaminate the resulting wavefield receiver gathers due to unidimensional assumption used to obtain the ghost operator. If we consider the real incidence angle regarding the offset trace in the receiver gather, calculating a bi-dimensional receiver ghost operator, these artifacts can disappear. This artifact is pointed by the number 4 arrow, in the Figure 9, while the real event is pointed by the number 3 arrow. The number 1 arrow refers to primary reflection in the upgoing and downgoing gathers. As we considered a normal incidence on horizontal water bottom reflector, the receiver ghost operator was built only for this unidimensional case, and good results were obtained for the near offset traces in the receiver gathers, coinciding with the interception zone (pointed by the number 2 arrow in the Figure 9) between the ghost operator artifact and the real ghost event, which provide the new receiver stack lines (Figure 10) verifying the robustness of the method proposed.
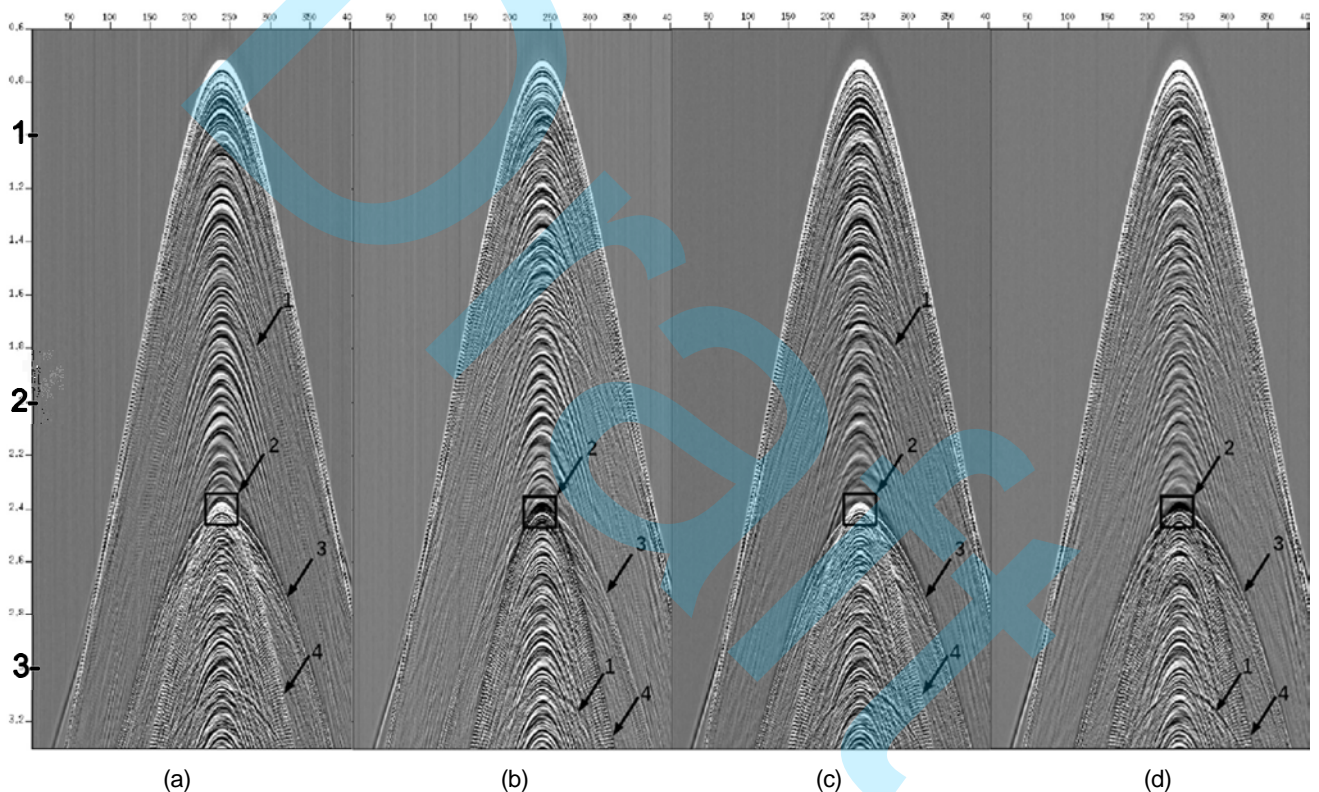

Figure 9 - *Long window deghosting receiver gathers. (a) Wiener-Levinson upgoing. (b) Wiener-Levinson downgoing. (c) IRLS upgoing. (d) IRLS downgoing. The vertical scale is in seconds.*

Deghosting – short window

Because the estimating short window is between water bottom and the first order multiple, the multiple energy does not generate the spurious conditions, and the notches does not appear on the component's amplitude spectra, thus the crossghosting step was excluded from filter calculation. The results show us similar quality in the gathers and the stacked receiver lines, with negligible differences
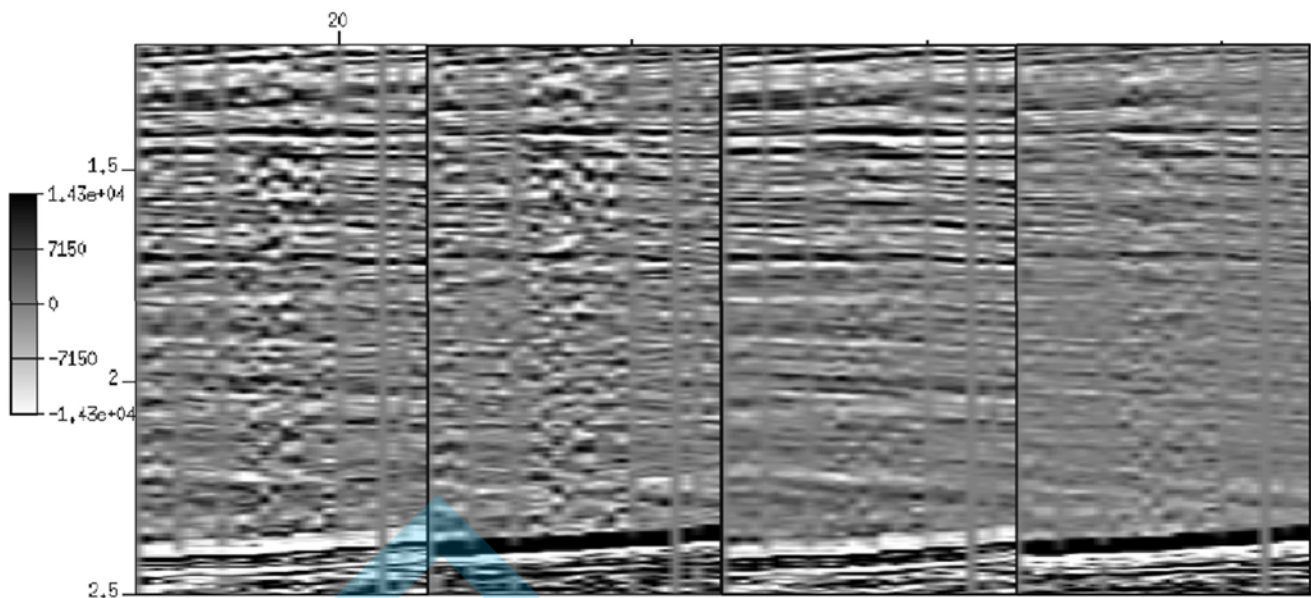
Figure 10 - *Details on long window deghosting receiver stack lines. From left to right are the Wiener-Levinson upgoing, the Wiener-Levinson downgoing, the IRLS upgoing and the IRLS downgoing.*

that enhance the raw amplitude spectra in useful frequency band in the IRLS upgoing gathers and reduce the raw amplitude level on high frequency band from quality control window (between the water bottom reflection and the first order multiple event) in the IRLS downgoing gathers, compared to Wiener-Levinson results. Due to the exclusion of the multiples from inside the short estimation window, the ghost operator artifact does not appear on the resulting receiver gathers.

Depeglegging

The depeglegging proceeding was applied with short window IRLS upgoing and downgoing wavefields as inputs. The results of applied IRLS predictive filter show us similar quality in the gathers and on their corresponding receiver stacked lines, when compared to Wiener-Levinson predictive filter results. The Figure 11 shows the data evolution on the receiver stack lines for the upgoing wavefield processing strategy, from the pressure and the particle velocity, which is represented by the integrated accelerometer receiver stack section, to the short windowed IRLS deghosted and the IRLS depegged receiver stack sections. Note that the first output was resulted with similar quality as the hydrophone section, although, in this case, remains just the peg-leg in the deghosted upgoing section. The resulting IRLS depegged section, obtained intermediate quality between the hydrophone and integrated accelerometer sections, showing a low level randon noised section, where it is noticed that the peg-leg became inconspicuous.
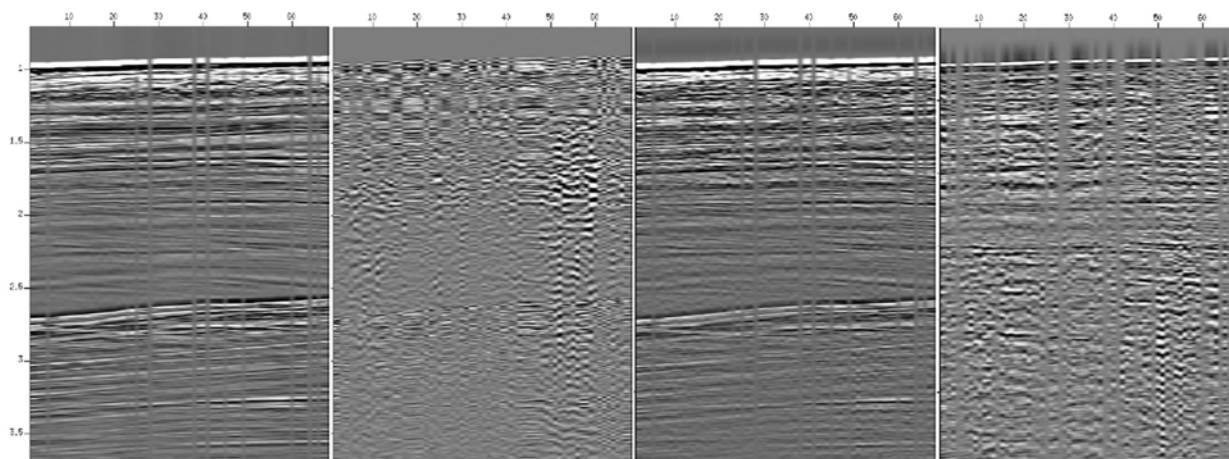
Figure 11 - *Data evolution on receiver stack lines. From left to right: input Hydrophone; input Vertical Integrated Accelerometer; output IRLS upgoing and output IRLS depegged. The vertical scale is in second.*

CONCLUSIONS

This work showed that filters based on L_1 norm are a good alternative to conventional Wiener-Levinson filters based on L_2 norm normally adopted in the treatment of ghost and peg-leg multiples present in seafloor seismic data. This was evident in the case where the multiples are present in the data window used to derive the coefficients of such filters.

The implementation of the L_1 Filter requires the solution of a non-linear system of equations, for this we present a mathematical procedure based on the IRLS method. This method has a higher computational cost, since it requires $n^3/3$ plus $2n^2$ float point operations to solve triangular systems using Cholesky in each iteration while the Wiener-Levinson filter requires only n^2 float point operations.

We recommend a previous processing preceding the PZ summation, as the designature and some noise attenuation. To perform the acoustic decomposition for deghosting, we must evaluate the size of the water column, to select the correct estimation window. When the estimation window contains multiple reflections, i.e., superposition between receiver ghost and peg leg, we recommend the application of the crossghosting operations before filter calculation. Thus, on shallow water bottom seismic data, it is difficult to determine an estimation window free of multiples; and on deep water bottom, the unidimensional solution for the ghost operator generates artifacts on receiver gather outputs.

The introduced method can be expanded to multi-dimensional case, if the correct incidence angle is calculated for each offset trace in the gather, so that the deterministic ghost operator can be correctly calculated, avoiding artifacts in outputs, as well as the filtering operation running to matrix or volumetric filter (multi-dimensional convolution).

REFERENCES

AMUNDSEN, L.; REITAN, A. Decomposition of multicomponent sea-floor data into upgoing and downgoing *P*- and *S*- waves. Geophysics, v. 60, p. 563–572, March–April 1995.

BERESFORD, G.; JANEX, G. A practical approach to OBC summation and geophone calibration in areas of shallow water and hard seafloor. In: 9th International Congress of the Brazilian Geophysical Society. SBGf, Salvador, BA, Brazil: [s.n.], 1996.

EDME, P.; SINGH, S. C. Receiver function decomposition of OBC data: theory. Geophysics, v. 177, p. 966–977, February 2009.

GOLUB, G. H.; VAN LOAN, C. F. Matrix Computation. 3rd. ed. Johns Hopkins: London, p. 159-176,207-213, 1996.

GUITTON, A.; VERSCHUUR, D. J. Adaptive subtraction of multiples using the L1-norm. Geophysical Prospecting, EAGE, v. 52, p. 27–38, 2004.

HUGONNET, P.; BOELLE, J. L.; HERRMANN, P.; PRAT, F.; LAFRAM, A. PZ summation of 3D WAZ OBS receiver gathers. In: 73rd EAGE Conference & Exhibition Incorporating SPE EUROPEC. Vienna, Austria: [s.n.], 2011.

LI, Z.-X.; LI, Z.-C.; LU, W. Multichannel predictive deconvolution based on the fast iterative shrinkage-thresholding algorithm. Geophysics, SEG, v. 81, n. 1, p. 17–30, January 2016.

MUIJS, R.; ROBERTSSON, J. O. A.; HOLLIGER, K. Data-driven adaptive decomposition of multicomponent seabed seismic recordings: Application to shallow-water data from the North Sea. Geophysics, v. 72, n. 6, p. V133–V142, November–December 2007.

OLIVEIRA, S. A. M.; LUPINACCI, W. M. L1 norm inversion method for deconvolution in attenuating media. Geophysical Prospecting, EAGE, p. 1–7, 2013.

PACAL, E. E.; STEWART, R. R.; BAYSAL, E.; YILMAZ O. Seismic Imaging with Ocean- Bottom Nodes (OBN): Mirror Migration Technique, SEG Technical Program Expanded Abstracts, August 2015.

ROSA, A. R. Análise do Sinal Sísmico. 2nd. ed. SBGf: Rio de Janeiro, RJ, Brazil. p. 306-313, 2018.

SCALES, J. A.; GERSZTENKORN, A. Robust methods in inverse theory. Inverse Problems, UK, n. 4, p. 1071–1091, March 1988.

SCHALKWIJK, K. M.; WAPENAAR, C. P. A.; VERSCHUUR, D. J. Adaptive decomposition of multicomponent ocean-bottom seismic data into downgoing and upgoing p- and s-waves. Geophysics, v. 68, p. 1091–1102, May–June 2003.

SOUBARAS, R. Ocean bottom hydrophone and geophone processing. In: SEG Technical Program Expanded Abstracts, p. 24-27, SEG, 1996.

WANG, Y.; GRION, S. PZ calibration in shallow waters: the Britannia OBS example. In: Las Vegas Annual Meeting. SEG: [s.n.], p. 1088–1092. 2008.

YILMAZ, O. Seismic Data Analysis - processing, inversion and interpretation of seismic data. 2nd. ed. USA: Doherty, SEG, v. 1. p. 159-270. 2001.

APPENDIX

The Iterative Reweighted Least Square method

The IRLS method is based on asymptotic approximation g(x) of the L_1 norm curve $f(x)$:

$$|x| = \overline{|x|^2 + \varepsilon^2},$$ (A1)

where ε is a small value (Figure A1).

Developing the derivative based on this approximation (equation A1), we found the nonlinear system of the IRLS method as

$$[M^T A M + \mu B] f_k = M^T A X$$ (A2)

which can be iteratively solved. Note that

$$A = diag \ [1/ \ \overline{\Delta^2 + \varepsilon}],$$ (A3)
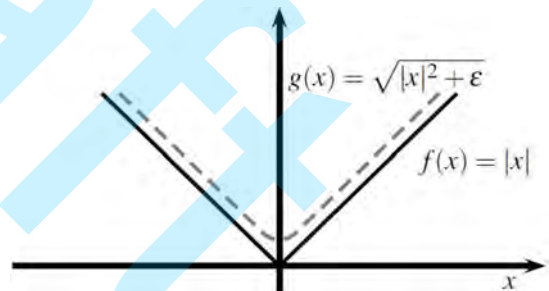
Figure A1 - *Asymptotic approximation g(x) which allow to differentiation of the L1 norm curve f(x).*

$$\Delta = |X - M f_k|,$$ (A4)

and

$$B = diag \ [1/(f_{k-1}^2 + \varepsilon)^{\frac{1}{2}}].$$ (A5)

The subscribed k is the iterating index; ε and μ are parameters, that can be respectively

described as the approximation accuracy controlling and the matrix regularizing to avoid division by zero (stabilizing the solution); M is the model, f_k is the filter and X is the data concerning the adaptive sum $X - Mf_k \approx 0$. The first iteration provides the least square solution (Oliveira and Lupinacci, 2013). To optimize it, we inserted the filter from the Wiener-Levinson algorithm to start the iterative method.